Blast Mitigation Analysis of Semi-Buried Structure

Goel, M.D.[1*] , Kumar, M.[2] and Matsagar, V.A.[3]

[1] Assistant Professor, Department of Applied Mechanics, Visvesvaraya National Institute of Technology (VNIT), Nagpur, India.
[2] M.Sc., Department of Civil Engineering, Indian Institute of Technology (IIT) Delhi, New Delhi, India.
[3] Associate Professor, Department of Civil Engineering, Indian Institute of Technology (IIT) Delhi, New Delhi, India.

ABSTRACT: Semi-buried structures are most commonly used at first line of defense along the border between two countries. This demands investigation of their dynamic behaviour under blast loading. Herein, a semi-buried structure with foam sandwiched walls and buttresses to reduce the effect of blast is analysed. The effect of provision of different configurations of buttresses and foam core between two layers of structural wall subjected to explosive loadings is investigated using ABAQUS/Explicit®. Modelling of semi-buried structure is carried out by employing shell elements and soil is modelled using frequency independent spring-dashpot-mass model. The foam core is modelled using brick elements with reduced integration and volumetric hardening. Effect of strain rate on structural steel is modelled by employing Johnson-Cook (J-C) model. Results indicate that geometry of buttresses and foam core type governs structural response to dynamic loading. It is observed that inner wall of the structure is protected by foam provided in between walls and helps in blast mitigation. Further, it is observed that design of such structures is dependent on the correct identification of buttresses type and isolation of inner wall of structure by provision of energy absorbing materials like foam.

Keywords: Buttresses Wall, Explosive Loading, Foam, Partially Buried Structure, Spring-Dashpot-Mass Model.

INTRODUCTION

Semi-buried structures are important part of protection facilities all around the world and are common in military setup. These structures need to be investigated for different threat levels and at the same time must be lightweight for their easy deployment along the frontier areas. Considering the situation, alternative designs and materials need to be explored for such structures without compromising safety and security of the occupants. It is well known that a buttress is a structure projecting from a wall and it serves to support the wall. Buttress walls and counterforts had been used by mankind for generations to provide reinforcement to main buildings which are subjected to unexpected tension and compression due to loads along the face of the structure. The use of buttress

* Corresponding author E-mail: mdgoel@gmail.com

walls was common on ancient buildings as a means of providing support against lateral forces. Buttress walls are similar in behaviour to counterfort walls except that buttress is positioned on the wall instead along the back as the case of counterforts. The vertical braces or stiffeners act as compression braces in such cases.

Research of structures subjected to blast loading is attaining attention and use of commercially available Finite Element (FE) packages is increasing due to practical difficulties in experimental investigations of structures subjected to blast loadings as reported by several authors (Hao, 2009; Bedon and Amadio, 2014; Shuaib and Daoud, 2015; Yang et al., 2015; Larcher et al., 2016; Abdollahzadeh et al., 2016). Physics of detonation process had already been studied in detail by several researchers (Brode, 1955; Henrych, 1979; Baker et al., 1983; Kingery and Bulmash, 1984; Kinney and Graham, 1985; TM 5-855-1, 1986; TM5-1300, 1990; Smith and Hetherington, 1994). Remennikov (2003) reported methodology for analysis of structures under blast and proposed application of FE modelling to analyse the structures. A review of blast wave interaction in different mediums was presented by Rajendran and Lee (2009). Later on, Goel et al. (2011, 2012a, 2013a, 2013c, 2015) studied performance of stiffened/sandwich structures and investigated response of different types of stiffeners and their positions along with the use of different types of materials under blast loading. Recently, Kumar et al. (2015) investigated dynamic semi-buried shelters under multiple blasts. They considered soil-structure interaction in their FE modelling. However, after detailed literature review, it is found that most of earlier investigations were focussed on underground structure like tunnels or ammunition storage facilities and limited investigations have been carried out for semi-buried structures under blast. Moreover, excessive vibrations due to blast

result in severe damage/dent to various secondary equipment. It is important to note that analysis, design and erection of such structures are dependent on ever advancing blast scenarios. Thus, recognition of various parameters for the dynamic response of such structures is of need. Further, it also requires investigation of the combination of materials and possible blast loading scenarios (Hao, 2009; Gebbeken et al., 2013; Bedon and Amadio, 2014; Shuaib and Daoud, 2015; Yang et al., 2015; Larcher et al., 2016; Aune et al., 2017; Figuli et al., 2017). Hence, an attempt is made herein to investigate the behaviour of semi-buried structure under non-contact explosive loading. For this purpose, a semi-buried structure with polymeric foam sandwiched walls and buttress is considered. The effect of provision of different configurations of buttresses and foam core between two layers of structural wall subjected to explosive loadings is investigated using ABAQUS/Explicit® (ABAQUS, 2013). The specific objective of the present investigation involves study of semi-buried structure for their displacements and stresses variation with the different configurations of the buttresses and foam material.

CONFIGURATION OF SEMI-BURIED STRUCTURE AND GEOMETRY OF BUTTRESSED WALL

Semi-buried structure with a dimension of 3 m × 3 m × 3 m is modelled. 30 mm thick steel plates are used for developing this structure. The geometrical design of this structure is of typical security surveillance unit used in defence set up. An approach route is provided to the structure from back side whereas, at top side, it has corrugated steel plates in the form of roof. Figure 1 represents geometry of structure for FE modelling. Moreover, for improved surveillance, structure geometry is chamfered at junction of walls (Figure 1). In

the present investigation, an un-buttressed structure (U1S) and buttressed structure with buttress wall of mild steel plates with thickness, t = 30 mm having different numbers, n on given face with inter-distance/distance, d from edge of the wall, width at bottom, b and height, h at surface of

the given face of the structure (Figure 2) has been analysed. It is to be noted that a total of six buttress configurations (B2S to B7S) are investigated and results are compared under blast loading. Sizes of different buttress wall considered in the herein are reported in Table 1.
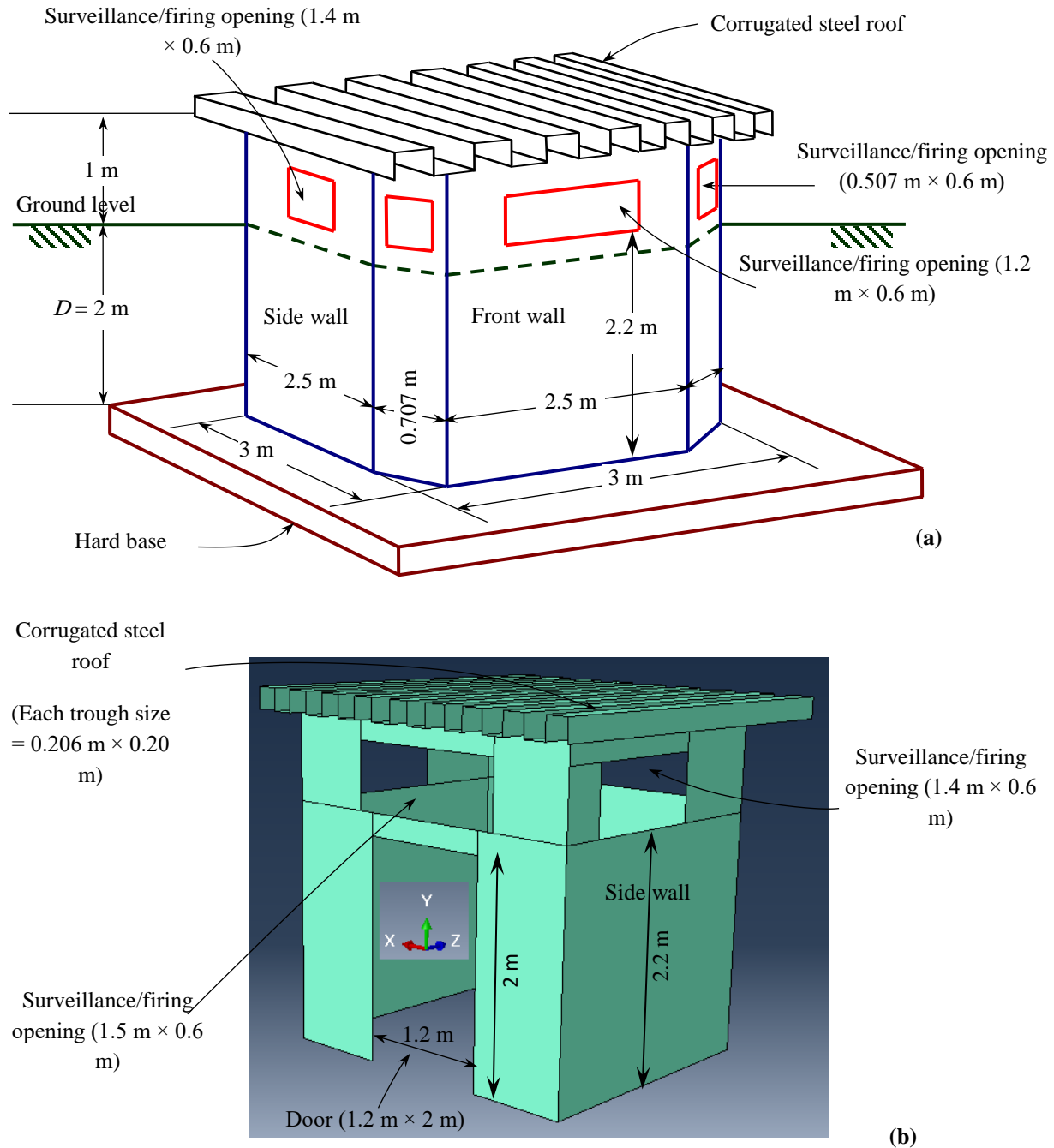

Fig. 1. Semi-buried structure geometry along with surveillance opening for a buried depth, D = 2 m: a) side and back view (sketch), b) front view (CAD model)

Table 1. Details of buttress configurations

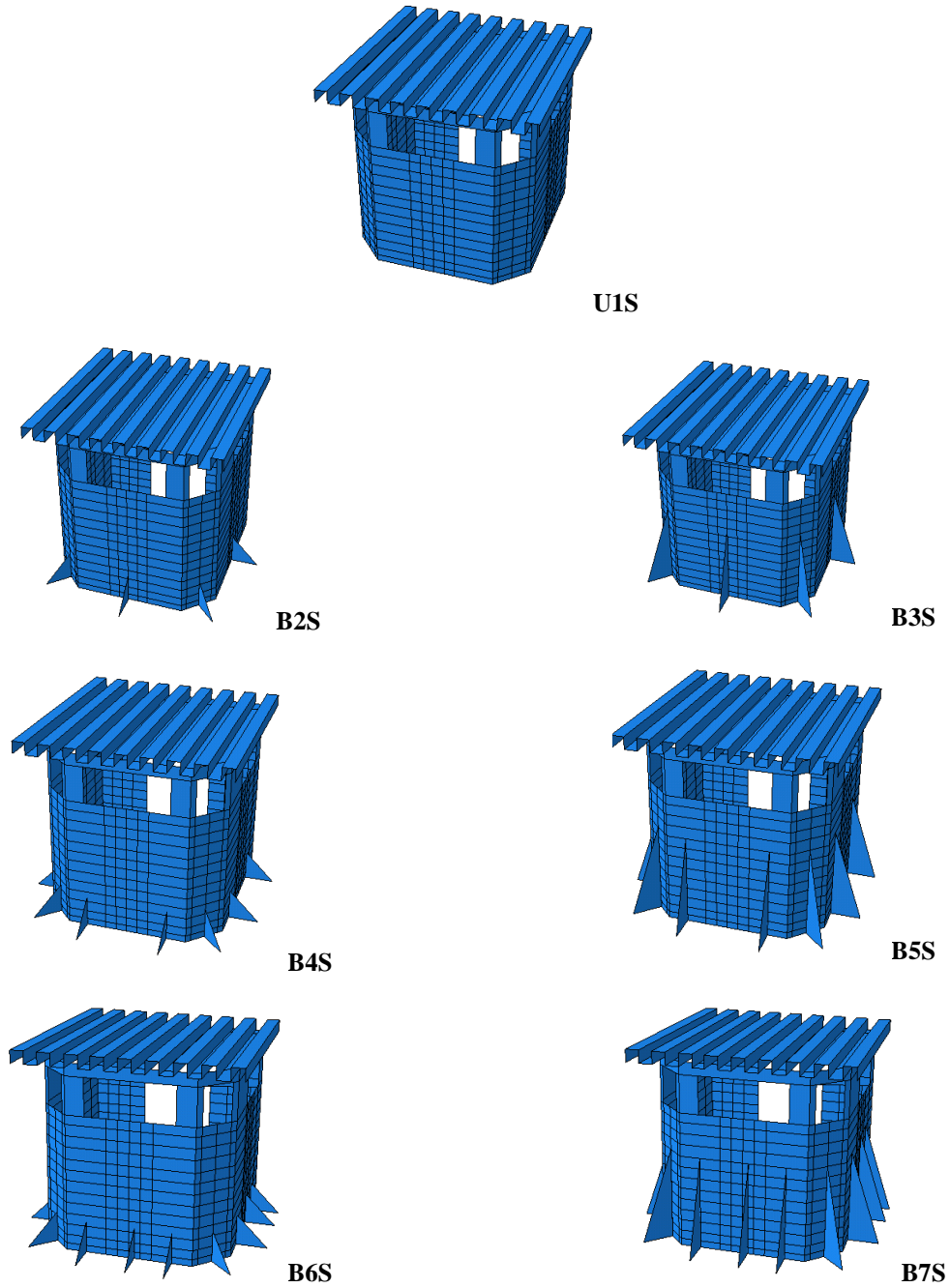|	Buttress Configurations						
	U1S	**B2S**	**B3S**	**B4S**	**B5S**	**B6S**	**B7S**
t (m)	0.03	0.03	0.03	0.03	0.03	0.03	0.03
n_{front}	0	1.00	1.00	2.00	2.00	3.00	3.00
d_{front} (m)	0	1.25	1.25	0.83	0.83	0.62	0.625
d_{side} (m)	0	1.25	1.25	0.83	0.83	0.62	0.625
b (m)	0	0.50	0.50	0.50	0.50	0.50	0.50
h/b	0	1.00	2.00	1.00	2.00	1.00	2.00

Fig. 2. Configurations of semi-buried structure assembly and buttresses

Friedlander's equation is used to define air blast (Goel et al., 2012b; Goel, 2015),

$$P(t) = P_{S0^+} \left(1 - \frac{t - t_a}{t_{0^+}} \right) \exp^{-b \frac{t - t_a}{t_{0^+}}} \qquad (1)$$

where $P(t)$: represents variation of pressure with time, peak incident pressure is represented by P_{S0^+}, positive blast wave duration is t_{0^+}, b: is coefficient of wave decay and arrival time of blast wave is represented by t_a. This Friedlander's equation (i.e. Eq. (1)) is commonly represented with a linear decay of pressure-with especially for positive blast wave duration (Goel et al., 2012b; Goel, 2015; Karlos et al., 2016) which is represented as,

$$P(t) = P_{S0^+} \left(1 - \frac{t}{t_{0^+}} \right) \qquad (2)$$

In the present investigation, P_{S0^+} and t_{0^+} is computed using expression given by Kinney and Grahm (1985). In the present investigation, blast scenario corresponding to an explosion of 10 kg of TNT (i.e. W) at a standoff distance of 2 m (i.e. R) is applied. This blast scenarios corresponds to a scaled distance i.e. Z ($= R/W^{1/3} = 0.93$ m/kg$^{1/3}$). This blast load can be applied using different methodologies such as: i) actual wave decay pulse as per Friedlander's equation, ii) Equivalent triangular pulse, iii) using ConWeP (Conventional Weapon) program function available in ABAQUS and iv) by using various fluid structure interaction techniques wherein air, soil, structure and explosive are modelled separately using different material models and they are made to interact with each other to depict the real scenario. The later one helps to realize the physics of the blast wave and its interaction with the structure/different media. It must be understood that generally, level of modelling and challenges keeps on increasing from (i) to (iv). Further, it is important to note that for present scenario, equivalent pulse method is applied considering its simplicity from application point of view which is commonly used by the structural designers in the field analysis.

STRESSES IN SOIL DUE TO BLAST

Stresses in soil are related to the decay of blast pressure with standoff distance and time. These radially expanding compressive blast waves propagate through soil medium and are expressed with the help of following equation (Wolf, 1989, 1997, Bowles, 1997) as:

$$P(t) = P_0 \, e^{-t/t_a} \qquad (3)$$

where P_0: is peak stress in soil and it is represented by:

$$P_0 = f \, \rho_c \, 160 \left[\frac{R}{W^{1/3}} \right]^{-n} \qquad (4)$$

where coupling factor is represented by f, acoustic impedance is ρ_c, and attenuation coefficient is represented by n. Herein, C is wave propagation velocity (Smith and Hetherington, 1994). Herein, f is 0.4 for zero scaled depth of burst (Smith and Hetherington, 1994; Drake and Little Jr. 1983). In this study, structure is surrounded by silt with acoustic impedance, ρ_c 9935 Pa/m/s, wherein, corresponding attenuation coefficient, n is 2.5. Propagation velocity, C, under the parameters considered herein is 500 m/s (Bowles, 1997). Various parameters of soil, used for modelling, are reported in Table 2.

Table 2. Material properties for soils

Soil Parameter	Values
Type of soil	Silt
Mass density, ρ (kg/m^3)	1650
Propagation velocity, C (m/s)	500
Acoustic impedance, ρ_c (Pa/m/s)	9935
Attenuation coefficient, n	2.5
Shear modulus, G (MPa)	53.57
Poisson's ratio, υ	0.4

Validation of Present FE Scheme

For improved confidence in numerical scheme and validation, results reported by Pereira et al. (2014) are utilized. Pereira et al. (2014) developed nonlinear Finite Element methods to evaluate the behaviour of unreinforced masonry wall against pressure loading. Dynamic analysis was performed using ABAQUS/Explicit® and numerical results were used to calibrate the model and close agreement amongst numerical model and experimental values was obtained. In the present investigation, wall is modelled as per Pereira et al. (2014) and material properties are used as presented by Pereira et al. (2014). Results computed by present FE scheme, are compared, in terms of displacement-time history with the results of Pereira et al. (2014). The results computed using present FE scheme is in well agreement of results reported by Pereira et al. (2014), thus validating the results of present FE scheme. Figure 3 shows the results of present numerical investigation with those reported by Pereira et al. (2014).

FINITE ELEMENT MODELLING

In the present investigation, three different materials are used for semi-buried structure i.e. steel, soil and foam material. Herein, dynamic response of the structure is obtained using ABAQUS/Explicit® (ABAQUS, 2013). Explicit time integration scheme is used for dynamic analysis and it satisfies the Courant time limit condition i.e., $\Delta t \leq l / c$, where l represents smallest element size and c represents sound wave speed. Quadratic and linear functions of volumetric strain rates are used with values of 1.2 and 0.06, respectively. The details of their FE modelling for various components are presented in this section.

Steel Modelling

Steel is used most commonly for design of structures against blast. For FE modelling of steel S4R elements with reduced integration and hourglass control are used (ABAQUS, 2013). In these elements, reduced integration is applied to remove the chances of shear and membrane locking, which is a common problem in blast modelling. Herein, fine (= 0.05), medium (= 0.1) and coarse mesh (= 0.15) are employed to verify the convergence of FE model. It must be noted that global mesh size controls the total number of elements in the part. The global mesh affect meshes at various levels (i.e. surface, volume, and inflation levels) and a scale factor multiplies other parameters to globally scale the FE model. Thus, global mesh size of 0.05, in the present investigation, represents that there will be there will be L/0.05 × B/0.05 numbers of element in the section considered. This function helps to generate a structured uniform mesh wherein mesh parameters are well taken care automatically by the built in algorithm of ABAQUS®. The numerical convergence is achieved at fine mesh which corresponds to a global mesh size of 0.05. All other investigations are carried out with this mesh configuration only. The material properties of structural steel are shown in Table 3. It is to be noted that strain rate effects in steel are most commonly expressed using Cowper-Symonds (C-S) or Johnson-Cook (J-

C) strain rate model. Recently, Vatani and Kiakojouri (2015) presented results of non-linear hollow I-core sandwich panel under air blast considering Cowper-Symonds strain rate model. However, in the present investigation, strain rate effect is applied using Johnson-Cook (J-C) model. This model defines dynamic stress, σ as (Johnson and Cook, 1983),

$$\sigma = \left(A + B\,\varepsilon^n\right)\left[1 + c\left(\log_e \dot{\varepsilon}^*\right)\right]\left(1 - T^{*m}\right) \qquad (5)$$

where A, B, c, m and n: are defined as material constants, ε: is the equivalent plastic strain and $\dot{\varepsilon}^* = \dot{\varepsilon}/\dot{\varepsilon}_0$: is dimensionless plastic strain rate for $\dot{\varepsilon}_0$ equal to 1 per second and $T^* = \left(T - T_{room}\right)/\left(T_{melt} - T_{room}\right)$. Table 3 shows J-C material parameters used in the present investigation by considering the strain rate effects but neglecting the temperature effects (Goel et al., 2011).

It is important to note that there exist various mechanical laws for modelling the steel in ABAQUS® as classical metal plasticity, cast iron plasticity and porous metal plasticity. To define yield and inelastic

flow of a metal at relatively low temperatures, classical metal plasticity is used wherein, loading is relatively monotonic and creep effects are unimportant. Further, cast iron plasticity model represents mechanical behaviour of gray cast iron, a material whose microstructure consisting of graphite flakes in a steel matrix. Finally, porous metal plasticity is more specifically used for materials wherein thin voids are less and relative density is > 0.9. Thus, there exist some voids in the materials which can be captured by this law. Further, the porous metal plasticity model describes materials that exhibit damage in the form of void initiation and growth (Amadio et al., 2017). In this study, emphasis was on the simple material modelling wherein least possible data for material is required which not the case for "Porous Metal Plasticity Model". It requires many parameters which many a times are difficult to obtain by simple tests. Hence, considering the restriction in the easy availability of parameters for porous plasticity, classical metal plasticity is applied in the present investigation.
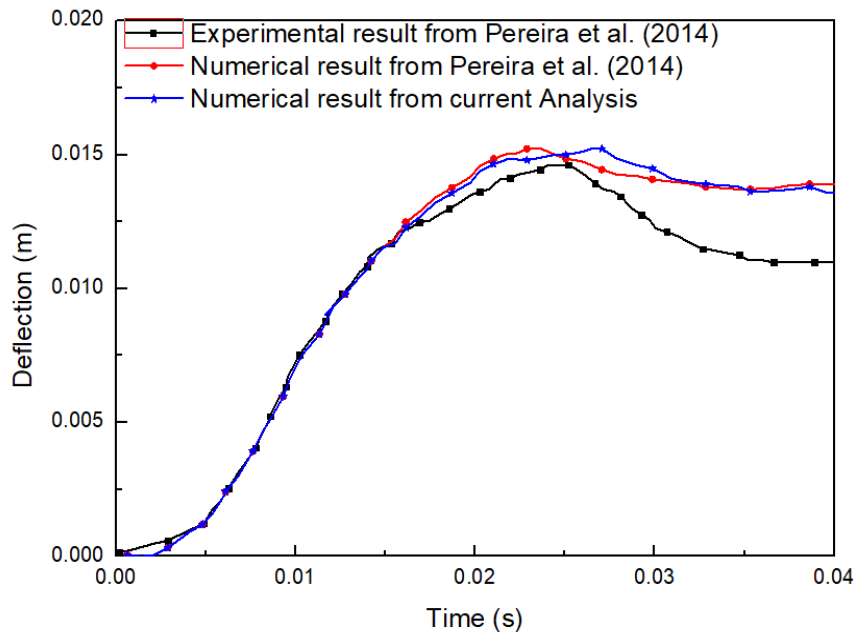

Fig. 3. Validation of present numerical scheme with numerical and experimental results of Pereira et al. (2014)

Table 3. Material properties for structural steel

Young's Modulus, E (GPa)	Poisson's Ratio, υ	Density, ρ (kg/m^3)	Static Yield Stress, f_y (MPa)
200	0.3	7850	250
	Johnson-Cook parameters		
A (MPa)	B (MPa)	n	C
360	635	0.114	0.075

Soil Modelling

It is to be noted that there exist several ways to model soil-structure interaction. Spring-dashpot model, in each degree-of-freedom, was proposed by Clough and Penzien (1975) to model the soil. Wolf (1989, 1997) reported a sophisticated model considering all motions. In his model, internal degrees-of-freedom were coupled with frequency independent coefficients. In the same year, Yang (1997) analysed a buried concrete shelter using visco-elastic soil model. Later on, Wang and Lu (2003) reported that simulation of explosion and soil-structure response requires a multi-phase soil model.

In the present investigation, soil-structure interaction is modelled using Wolf's frequency independent model (Wolf, 1989, 1997). Inertial and damping effects of soil during blast were included in addition to static spring stiffness. This was modelled in each degree-of-freedom by spring-dashpot model (Wolf, 1989, 1997; Bowles, 1997). Recently Seyedan and Seyedi (2015) studied the significance of soil compaction on blast resistant behaviour of underground structures. However, in this investigation, soil is considered as a continuum body for all motions and three internal degrees-of-freedom at all the discretized nodes of structure (Wolf, 1989, 1997). The structure is analysed for three buried depth conditions i.e. $D = 0.67$ m, 1.33 m and 2 m under a constant scaled distance of 0.93 m/kg$^{1/3}$. In the present investigation, silt is used as a soil material, adjoining the semi-buried structures' walls. The characteristics of silty soil used in this investigation are already reported in Table 2 (Bowles, 1997).

Foam Modelling

Foam materials exhibit characteristics of absorbing high energy; therefore, these materials had been used as core in sandwich structures to isolate the primary structures from blast load applied on secondary structures (Goel et al., 2011, 2012a, Yang et al., 2015). Foam core is a cladding sandwiched in between metal cover plates of primary and secondary structure. When subjected to an explosion, maximum impact is transferred from front wall to foam core which undergoes large deformation and thus, absorbs maximum energy and attenuates the impact and blast loads by means of cell collapse mechanism. The rear wall behind the foam core is then protected and overall impact of the blast load is reduced (Goel et al., 2011, 2012a, 2013b, 2013c, 2014, 2015).

In the present investigation, constitutive model developed by Deshpande and Fleck (2000) is used for modelling of foams. There are two variations of this constitutive model as: i) volumetric hardening model and ii) isotropic hardening model. Both models use a yield surface wherein, deviatoric stress is elliptical and it depends on pressure stress in the meridional plane. Volumetric hardening model usually shows a different response in compression and tension as reported by experiments carried out by Deshpande and Fleck (2000). Plastic response for pure shear is truly represented by this model. Further, for other loading leading to negative pressure state (i.e. uniaxial tension) and positive pressure state, this model is accurate. Symmetric behaviour in tension and compression is used by isotropic hardening model and yield surface evolution is represented by an equivalent plastic strain

(Deshpande and Fleck, 2000).

In the present investigation, two different types of foam materials i.e. Dytherm 2.5 (D2.5) and Polyurethane (PU) as foam core with thicknesses, $c = 100$ mm are used as shown in Figure 4 along with the blast pulse. An 8-node linear brick element (C3D8R) with hourglass control and reduced integration is used to model foam material. Young's modulus, E and elastic Poisson's ratio, ν are used to defined elastic behaviour. Properties of two foam core material i.e. Dytherm 2.5 (D2.5) and Polyurethane (PU), used in present investigation, are reported in Table 4. It is further to be noted that initial yield behaviour of this foam model is governed by k. This is the ratio of initial yield stress in uniaxial compression to initial yield stress in hydrostatic compression), σ_c^0 / p_c^0 and k_t, the ratio of yield stress in hydrostatic tension to initial yield stress in hydrostatic compression, p_t / p_c^0. Figure 5 shows stress-

strain curves of foams used in the present investigation. Friction coefficient of 0.2 for Dytherm 2.5 and 0.3 for Polyurethane is used to define contact interaction between steel plates and foam core.

RESULTS AND DISCUSSIONS

Effect of Buttress Configurations

In the present investigation, six different types of buttresses are investigated. The buttress numbers and their configurations are based on the concept of addition of equal mass to the un-buttressed configuration for comparing their dynamic behaviour under same mass. The applied blast load-time history over the semi-buried structure due to blast load of 10 kg TNT at 2.0 m standoff is reported in Figure 4. This figure also shows the Friedlander's wave profile for the same loading conditions and idealized triangular blast profile considered in the present investigation.
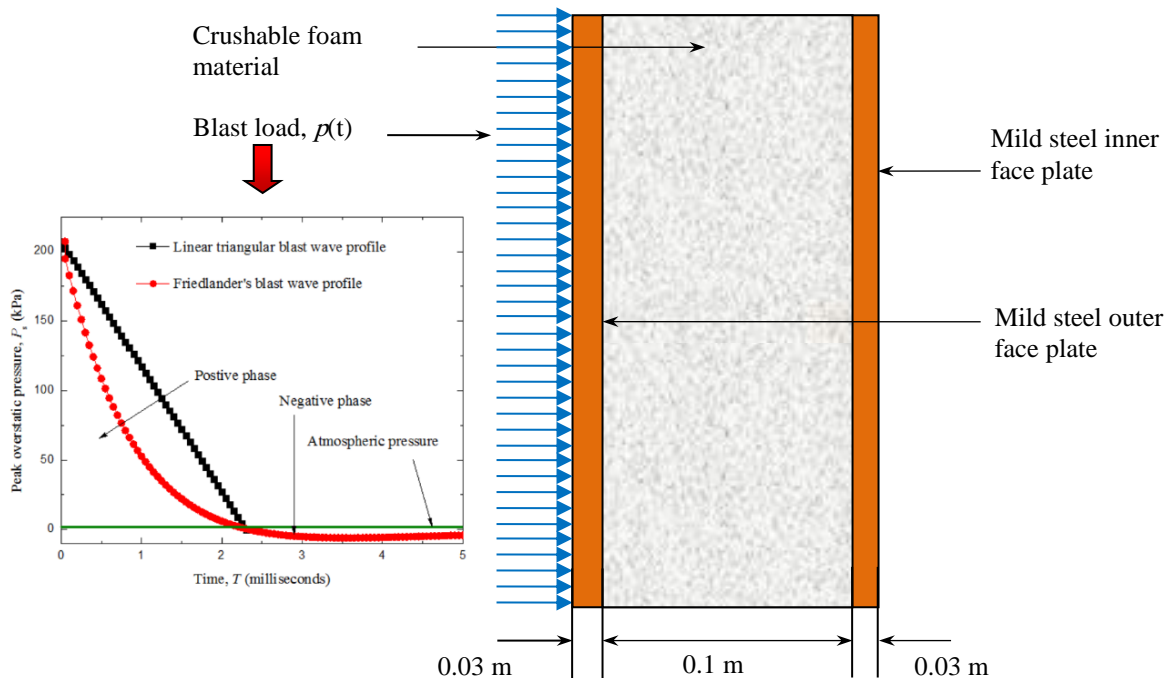

Fig. 4. Schematic of foam core and wall of semi-buried structure along with application of uniform equivalent triangular blast pulse

Table 4. Material properties of crushable foam material

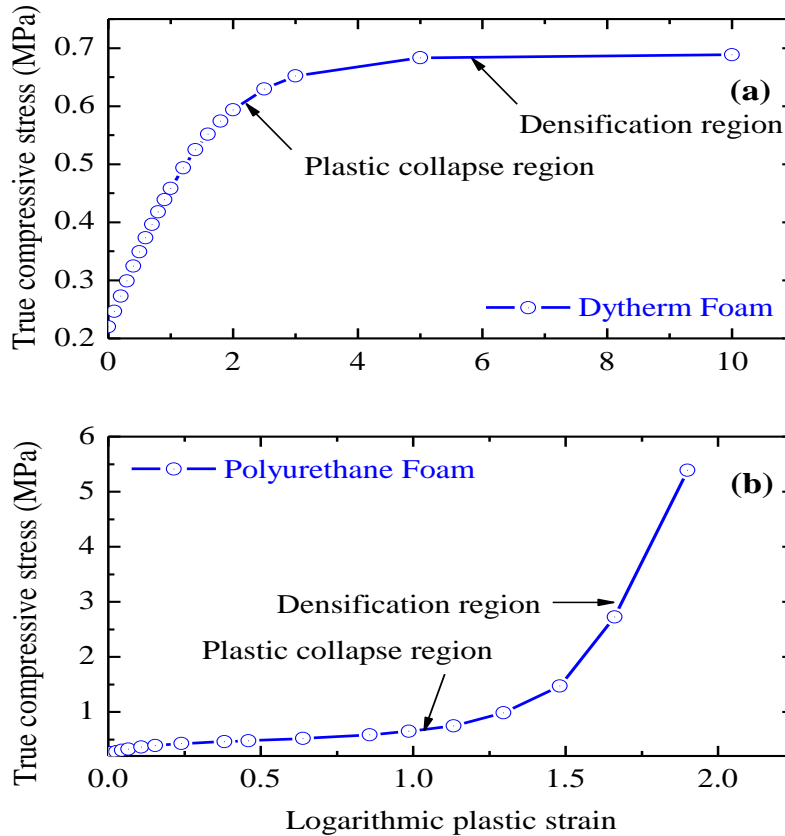| Properties	Dytherm 2.5 (D2.5)	Polyurethane (PU)
Young's modulus, E (MPa)	3.0	7.5
Poisson's ratio, ν	0.0	0.0
Density, ρ (kg/m^3)	100	60
Initial yield stress in uniaxial compression σ_c^0 (MPa)	0.22	0.2
Yield stress in hydrostatic tension p_t (MPa)	0.02	0.02
Yield stress in hydrostatic compression p_c^0 (MPa)	0.2	0.2
$k = \sigma_c^0 / p_c^0$	1.1	1.0
$k_t = p_t / p_c^0$	0.1	0.1
Plastic Poisson's ratio, ν_p	0	0
Friction coefficient, f	0.3	0.2

Fig. 5. Strain hardening behavior of foams under compression: a) Dytherm 2.5 and b) Polyurethane

Based on FE analysis, Figure 6 shows displacement-time history of semi-buried structure with different buttress configurations considered in the present investigation. The peak displacement un-buttressed and buttressed configuration i.e. B2S to B7S, is found to be 69.43 mm and 75.24 mm, 63.71 mm, 69.37 mm, 57.90 mm, 71.1 mm, and 59.90 mm, respectively. From this, it can be observed that B3S, B4S, B5S, and B7S buttress configurations results in lower peak displacements as compared to un-buttressed structure whereas, B2S and B6S configurations shows higher peak

displacement as compared to un-buttressed structure for all other conditions being same. This may be attributed to the lower stiffness of B2S and B6S configurations in comparison with other buttresses configurations. Further, based on their geometry and location other buttresses configurations results in effective distribution of stiffness which results in higher mitigation of blast loads. Thus, it can be concluded that not only size and shape of the buttresses but their effective placement also governs the response under blast loading. Figure 7 shows non-dimensional stress parameter (i.e. ratio of von-Mises stress to yield stress) in structure and buttress to blast load of 10 kg TNT at 2.0 m standoff considered in the present investigation. From this figure, it can be noted that not all the buttress configurations results in reduction of stresses in semi-buried structure. Although, there is significant stress reduction in all the structures with the provision of buttresses but in buttresses itself, stress concentration is observed. Moreover, it can be observed that B3S and B7S buttresses shows higher stresses, whereas, all other buttresses

configurations resulted in lower stresses in comparison with un-buttressed structure. The reason for this behaviour may be attributed to the fact of localization of stress at joints of buttresses (in case of B3S and B7S configurations) with the main structure. And this is the precise reason for such behaviour of B3S and B7S buttress configuration in comparison with other buttresses.

Effect of Crushable Foam Material

In the present investigation, two type of foam material is used for blast isolation and its mitigation. Dynamic analysis has been carried out to compute peak displacements and maximum von-Mises stresses on inner face panel along the direction of applied blast load. Observation points are selected such that they coincide with centre point at sill level of opening on front side of structure which is at 2.1 m from the bottom of structure (Figure 1). The structure, semi-buried in silt, has been subjected to blast loading with $Z = 0.93$ m/kg$^{1/3}$. The FE analysis is carried out using ABAQUS/Explicit® (ABAQUS, 2013).
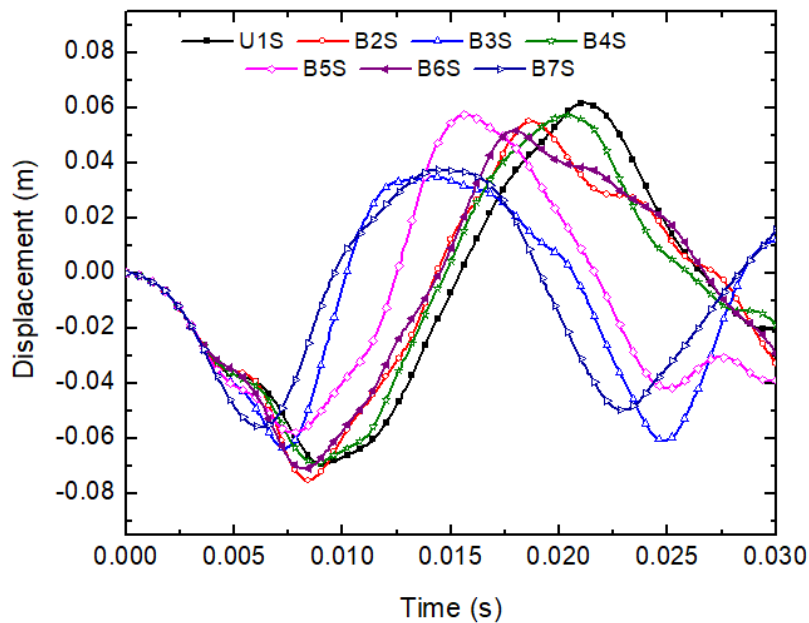

Fig. 6. Displacement-time history of buttress reinforced semi-buried structure subjected to blast load of 10 kg TNT at 2.0 m standoff
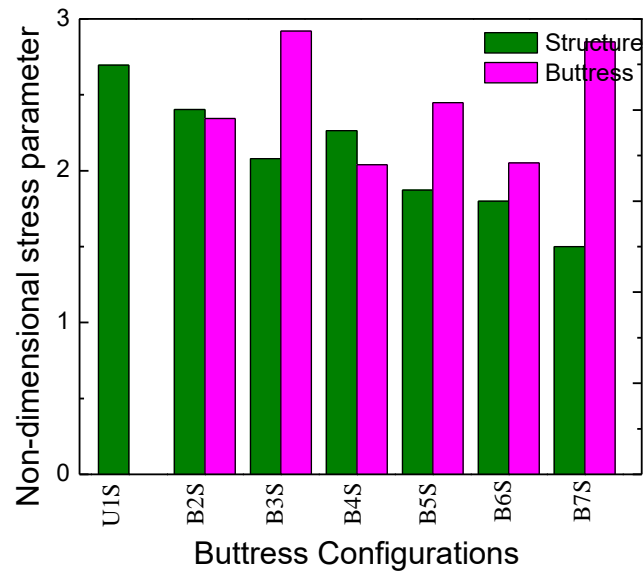
Fig. 7. Non-dimensional stress parameter (i.e. ratio of von-Mises stress to yield stress) in structure and buttress to blast load of 10 kg TNT at 2.0 m standoff

In the first analysis, inner structure of single mild steel panels (MS) isolated using foam material i.e. Dytherm 2.5 (D2.5) and Polyurethane (PU) with outer mild steel face panel, as covering sheet panel, has been analysed under a scaled distance i.e. $Z = 0.93$ m/kg$^{1/3}$ with different buried depth. Figure 8 shows peak displacement of structure with varying buried depth for different combinations of single mild steel panel (MS) and foam cores considered in the present investigation. It is evident from this figure that provision of foam cores results into significant reduction in peak displacement in comparison with only steel panels for all the buried depth and two different foam types considered herein. Further, it is interesting to note that, peak displacement, for a buried depth 0.5 m, is higher, even with the provision of foam cores, in comparison with the structure at ground. However, with the increase in buried depth (≥ 1 m) peak displacement is significantly lower than the structure at ground. Further, at buried depth of 2 m, it is observed that there is almost insignificant displacement in the structure under the blast considered in the present

investigation. At buried depth of 2 m, effect of foam core is almost insignificant for the blast scenario considered herein. The reason for such behaviour may be attributed to the effect of soil damping which results in reduced displacement by absorbing the most of blast energy.

Figure 9 shows the maximum von-Mises stress in structure with varying buried depth for different combinations of single mild steel panel (MS) and foam cores considered in the present investigation. The behaviour is similar to the case of peak displacement as discussed above. However, it can be observed from this analysis, that PU foam exhibits higher energy absorption as evident from lower peak displacements and von-Mises stresses in comparison with the Dytherm foam. For surface blast at zero depth, displacement and von-Mises stress for single mild steel panel (without foam core) are observed as 51.10 mm and 518 MPa, respectively. Whereas, for sandwich panels with Dytherm 2.5 and polyurethane (PU) as foam core, displacement and von-Mises stress are observed as 29.69 mm, 384.50 MPa and 26.60 mm, 340.30 MPa, respectively.

Thus, Dytherm 2.5 results in reduction of peak displacement by 42% and stresses by 26% in comparison with single steel panel. Whereas, polyurethane results in 48% lower displacement and 35% lower stresses for all other conditions being same. Further, based on the observed trends of displacement and stresses, this analysis shows that PU foam is more efficient as core material in reduction of peak displacements and von-Mises stresses at all depths considered herein. Hence, it is concluded that displacement and stress reduction is inversely proportional to the foam core density and buried depth.

In the second analysis, response of structure buried in silt by a depth of 1.5 m with Polyurethane (PU) core under varying scaled distance has been carried out. Displacement of inner and outer face plate at 0.5 milliseconds under blast of different scaled distances, with silt as surrounding soil medium, is reported in Figure 10. It can be observed from this figure, that displacement increases with the decrease in scaled distance and displacement of outer face plate is more than inner face due to high compressibility of polyurethane foam. It is observed that cross-section of foam, in between two observations point, is always in compression. The reason for such behaviour may be attributed to the fact that for the structure subjected to a nearby explosion, maximum impact is transferred from front face panel to the foam core which undergoes large deformation and thus, absorbs maximum energy and attenuates blast loads by means of cell collapse mechanism. The inner face panel behind the foam core is then protected and overall impact of the blast load is reduced. Further, with the increase in scaled distance, peak displacement is decreasing and at scaled distances > 3 m/kg$^{1/3}$, displacement is almost negligible for the semi-buried structure considered in the present investigation. Hence, it is concluded that geometry of buttresses and foam core type governs the blast mitigation of such structures. Further, it also depends on isolation of inner wall of structure by foam, buried depth and scaled distance. All these parameters together govern the behaviour of such structures under blast loading with all other conditions being same.
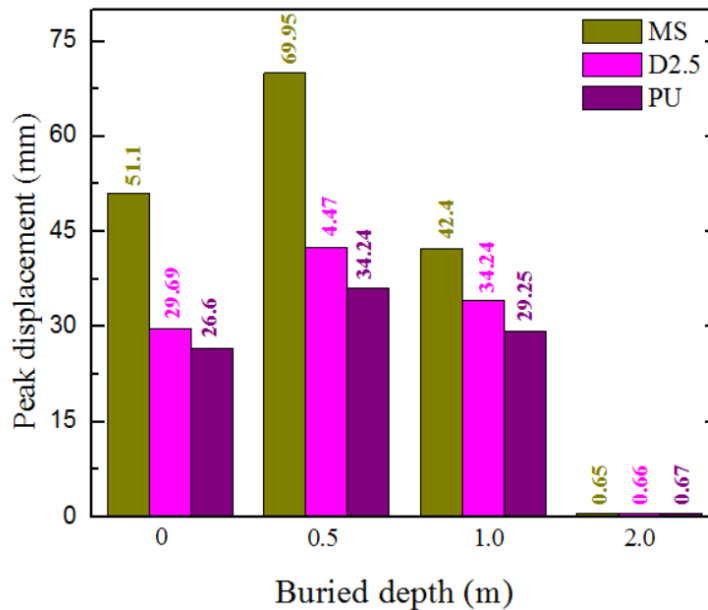

Fig. 8. Variation of peak displacement of outer face plate with buried depth and different foam cores for blast of 10 kg TNT at 2 m standoff in silt
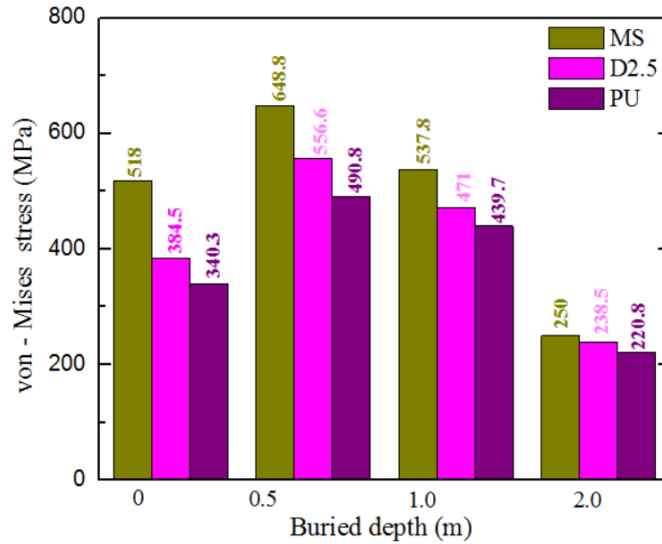
Fig. 9. Variation of von-Mises stress with buried depth and different foam cores for blast of 10 kg TNT at 2 m standoff in silt
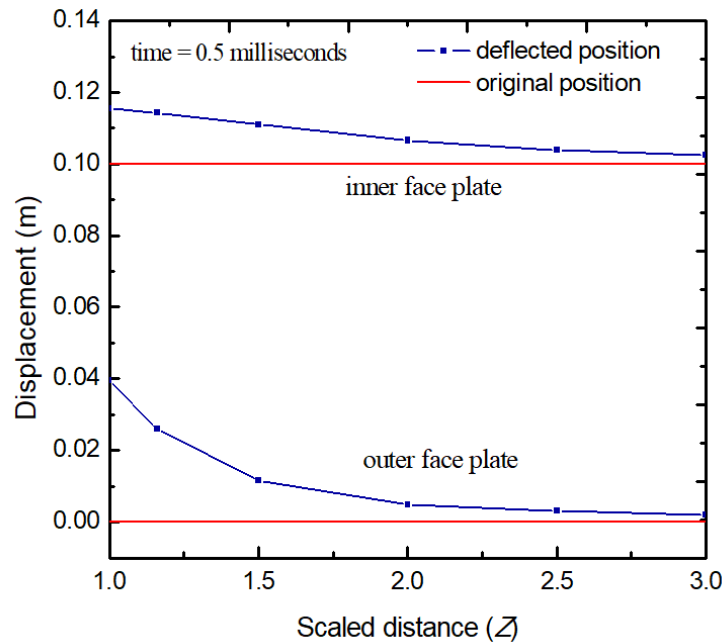

Fig. 10. Displacement of inner and outer face plate at 0.5 milliseconds with polyurethane core cladding due to blast of different scaled distance with silt as surrounding soil medium

CONCLUSIONS

The specific objective of the present investigation involves study of semi-buried structure for their displacements and stresses variation with the different configurations of the buttresses and foam material. Herein, effect of geometry of different buttresses wall provided monolithically to structure subjected to nearby blast loading is investigated. Based on this FE investigation, following conclusions are drawn:

1) Buttress walls can be effectively used as reinforcement to semi-buried structure and these walls results in considerable reduction of peak displacement and von-Mises stress.

2) Based on this investigation, it is observed that it is important to choose proper size and position of the buttress wall as all the configurations do not results into reduction of peak displacement and von-Mises stress.

3) Foam core between two panels leads to isolation of inner panel from direct effects of blast loading and results in lower pressure transferred to inner wall.

4) PU foam is more effective for the blast scenario applied in this investigation.

5) With the increase in buried depth there is significant reduction in peak displacement and stresses.

6) Displacement and von-Mises stress reduction are inversely proportional to density of core foam core and buried depth of the structure.

7) Stress concentration is observed at the edge of buttresses and it's joint with semi-buried structure wall for Dytherm foam core. This is the main reason for lower reduction of von-Mises stress in case of Dytherm foam core.

8) With increasing scaled distance, peak displacement is decreasing and at scaled distances > 3 m/kg$^{1/3}$, displacement is almost negligible for the semi-buried structure considered herein.

REFERENCES

ABAQUS/Explicit® (2013). *User's manual*, Dassault Systemes Simulia Corporation, France.

Abdollahzadeh, G.R., Nemati, M. and Avazeh, M. (2016). "Probability assessment and risk management of progressive collapse in strategic buildings facing blast loads", *Civil Engineering Infrastructures Journal*, 49(2), 327-338.

Amadio, C., Bedon, C., Fasan, M. and Pecce, M.R. (2017). "Refined numerical modelling for the structural assessment of steel-concrete composite beam-to-column joints under seismic loads", *Engineering Structures*, 138, 394-409.

Aune, V., Valsamos, G., Casadei, F., Larcher, M., Langseth, M. and Børvik, T. (2017). "Numerical study on the structural response of blast-loaded thin aluminium and steel plates", *International Journal of Impact Engineering*, 99, 131-144.

Baker, W.E., Cox, P.A., Westine, P.S., Kulesz, J.J. and

Strehlow, R.A. (1983). *Explosion hazards and evaluation*, Elsevier Scientific Publishing Company, New York, U.S.A.

Bedon, C. and Amadio, C. (2014). "Exploratory numerical analysis of two-way straight cable-net façades subjected to air blast loads", *Engineering Structures*, 79, 276-289.

Bowles, J.E. (1997). *Foundation analysis and design*, McGraw-Hill, Singapore.

Brode, H.L. (1955). "Numerical solutions of spherical blast waves", *Journal of Applied Physics*, 26(6), 766-75.

Clough, R.W. and Penzien, J. (1975). *Dynamics of structures*, McGraw Hill, New York, U.S.A.

Deshpande, V.S. and Fleck, N. A. (2000). "Isotropic constitutive model for metallic foams", *Journal of the Mechanics and Physics of Solids*, 48(6-7), 1253-1276.

Drake, J. L. and Little Jr., C.D. (1983). "Ground shock from penetrating conventional weapons", ADP001706, *Army Engineer Waterways Experiment Station Vicksburg,* Mississippi, Colorado, U.S.A.

Figuli, L., Bedon, C., Zvaková, Z. and Kavický, V. (2017). "Dynamic analysis of a blast loaded steel structure", *Procedia Engineering*, 199, 2463-2469.

Gebbeken, N., Huebner, M., Larcher, M., Michaloudis, G. and Pietzsch, A. (2013) "Concrete and reinforced concrete structures subjected to explosion and impact", *Beton-Und Stahlbetonbau*, 108(8), 515-527.

Goel, M.D., Matsagar, V.A. and Gupta, A.K. (2011). "Dynamic response of stiffened plates under air blast", *International Journal of Protective Structures*, 2(1), 139-155.

Goel, M.D., Chakraborty, T. and Matsagar, V.A. (2012a). "Dynamic response of steel-sand composite stiffened plates under impulsive loading", *Journal of Battlefield Technology*, 15(3), 1-7.

Goel, M.D., Matsagar, V.A., Gupta, A.K. and Marburg, S. (2012b). "An abridged review of blast wave parameters", *Defence Science Journal*, 62(5), 300-306.

Goel, M.D. and Matsagar, V.A. (2013a). "Blast resistant design of structures", *Practice Periodical in Structural Design and Construction*, American Society of Civil Engineers (ASCE), 19(2), 04014007.

Goel, M.D., Matsagar, V.A., Gupta, A.K. and Marburg, S. (2013b). "Strain rate sensitivity of closed cell aluminum fly ash foam", *Transactions of Nonferrous Metals Society of China*, 23, 1080-1089

Goel, M.D., Matsagar, V.A., Marburg, S. and Gupta, A.K. (2013c). "Comparative performance of

stiffened sandwich foam panels under impulsive loading", *Journal of Performance of Constructed Facility*, American Society of Civil Engineers (ASCE), 27(5), 540-549.

Goel, M.D., Matsagar, V.A. and Gupta, A.K. (2014). "Blast resistance of stiffened sandwich panels with aluminum closed cell foam", *Latin American Journal of Solids and Structures*, 11(13), 2497-2515.

Goel, M.D. (2015). "Blast: Characteristics, loading and computation, An overview", *Advances in Structural Engineering Mechanics*, Vasant Matsagar (ed.), 1, 417-434.

Goel, M.D., Matsagar, V.A. and Gupta, A.K. (2015). "Blast resistance of stiffened sandwich panels with aluminum cenosphere syntactic foam", *International Journal of Impact Engineering*, 77, 134-146.

Hao, H. (2009). "Numerical modelling of masonry wall response to blast loads", *Australian Journal of Structural Engineering*, 10(1), 37-52.

Henrych, J. (1979). *The dynamics of explosion and its use*. Elsevier Scientific Publishing Company, Amsterdam, Norway.

Johnson, G.R. and Cook, W.H. (1983). "A constitutive model and data for metals subjected to large strains, high strain rates and high temperatures", *Proceedings of the 7th International Symposium on Ballistics,* The Hague, Netherlands.

Karlos, V., Solomos, G. and Larcher, M. (2016). "Analysis of the blast wave decay coefficient using the Kingery–Bulmash data", *International Journal of Protective Structures*, 7(3), 409-429.

Kingery, C.N. and Bulmash, G. (1984). "*Airblast parameters from TNT spherical air burst and hemispherical surface burst*", US Army Armament and Development Center, Ballistic Research Laboratory.

Kinney G. and Graham K. (1985). *Explosive shocks in air*, Springer-Verlag, New York, U.S.A.

Kumar, M., Goel, M.D., Matsagar, V.A. and Rao, K.S. (2015). "Response of semi-buried structures subjected to multiple blast loading considering soil-structure interaction", *Indian Geotechnical Journal*, 45(3), 243-253.

Larcher, M. Arrigoni, M., Bedon, C., van Doormaal, J.C.A.M., Haberacker, C. Hüsken, G., Millon, O., Saarenheimo, A., Solomos, G., Thamie, L., Valsamos, G., Williams, A. and Stolz, A. (2016). "Design of blast-loaded glazing windows and facades: A review of essential requirements towards standardization", *Advances in Civil Engineering*, 2016, 1-14.

Pereira, J., Campos, J. and Lourenco, P. (2014). "Experimental study on masonry infill walls under blast loading", *Proceedings of the 9th International Masonry Conference*, Guimarães, Portugal.

Rajendran, R. and Lee, J.M. (2009). "Blast loaded plates", *Marine Structure,* 22, 99-127.

Remennikov, A.M. (2003). "A review of methods for predicting bomb blast effects on buildings", *Journal of Battlefield Technology*, 6(3), 5-10.

Seyedan, M.J. and Seyedi, H.E. (2015). "Significance of soil compaction on blast resistant behaviour of underground structures: a parametric study", *Civil Engineering Infrastructures Journal*, 48(2), 359-372.

Shuaib, M. and Daoud, O. (2015). "Numerical modelling of reinforced concrete slabs under blast loads of close-in detonations using the Lagrangian approach", *Journal of Physics*: *Conference Series*, 628(1),1-8.

Smith, P.D. and Hetherington, J.G. (1994). *Blast and ballistic loading of structures,* Butterworth Heinemann Limited, U.K.

U.S. Department of the Army (1986). "*Fundamentals of protective design for conventional weapons*", Technical Manual, TM 5-855-1, Washington D.C., U.S.A.

U.S. Department of the Army, Navy and Air Force (1990). "*The design of structures to resist the effects of accidental explosions*", Technical Manual, TM 5-1300, Washington DC, U.S.A.

Vatani, O.A. and Kiakojouri, F. (2015). "Non-linear dynamic analysis of steel hollow I-core sandwich panel under air blast loading", *Civil Engineering Infrastructures Journal*, 48(2), 323-344.

Wang, Z. and Lu, Y. (2003). "Numerical analysis on dynamic deformation mechanism of soils under blast loading", *Soil Dynamics and Earthquake Engineering*, 23(8), 705-714.

Wolf, J.P. (1989). "Soil-structure-interaction analysis in time domain", *Nuclear Engineering and Design*, 111(3), 381-393.

Wolf, J.P. (1997). "Spring-dashpot-mass models for foundation vibrations", *Earthquake Engineering and Structural Dynamics*, 26(9), 931-949.

Yang, F., Niu, W., Jing, L., Wang, Z., Zhao, L. and Ma, H. (2015). "Experimental and numerical studies of the anti-penetration performance of sandwich panels with aluminum foam cores", *Acta Mechanica Solida Sinica*, 28(6), 735-746.

Yang, Z. (1997). "Finite element simulation of response of buried shelters to blast loadings", *Finite Elements in Analysis and Design*, 24(3), 113-132.